

**COMPARISON OF AUTHIGENIC MINERALS IN SANDSTONES AND
INTERBEDDED MUDSTONES, SILTSTONES AND SHALES, EAST BERLIN
FORMATION, HARTFORD BASIN, USA**

Wolela Ahmed

Department of Petroleum Operations, Ministry of Mines, P.O. Box 486, Addis Ababa, Ethiopia

(Received November 28, 2005; June 19, 2006)

ABSTRACT. The East Berlin formation consists mainly of alternating sequences of fluvialite, lacustrine and playa sediments. Diagenetic sequences reconstruction revealed the same range of authigenic minerals in the studied sandstones and the interbedded fine-grained sediments (mudstones and siltstones). This indicates that the diagenetic processes that took place in the sandy facies also took place in fine-grained sediments. Mechanically infiltrated clays, grain-coating clay/hematite, quartz and feldspar overgrowths, carbonate cements and pore-filling and pore-lining clay minerals that precipitated in the sandy facies also precipitated in the fine-grained sediments. The abundance of authigenic minerals in decreasing order include: sandstone > siltstone > mudstone > shale. Except minor amounts of authigenic illite-smectite and illite, the shaly facies dominated by detrital clay, carbonate, quartz and feldspars framework grains. Authigenic minerals such as quartz, albite and K-feldspar are absent in the shaly facies, possibly related to early destruction of porosity. The lacustrine sandstones, siltstones and mudstones followed marine diagenetic trend, whereas playa and fluvialite sandstones, siltstones and mudstones followed red bed diagenetic trend. Mechanically compacted mudstones, siltstones and shales expelled large volume of mineralized pore water, which might migrated into the sandstone-rich section. Part of the ions for the precipitation of quartz overgrowths and carbonate cements in the sandy facies possibly contributed from the interbedded siltstones, mudstones and shales facies.

KEY WORDS: Authigenic minerals, Mudstone, Sandstone, Siltstone, East Berlin formation, Hartford Basin

INTRODUCTION

The East Berlin formation consists mainly of alternating sequences of fluvialite, lacustrine and playa sediments [1]. The formation was considered for case studies to understand the diagenetic minerals in fluvialite, playa and lacustrine sandstones and the interbedded fine-grained sediments whether they follow the same or different diagenetic trends. The major factors which control diagenesis of sandstone and other clastic sediments include: temperature, pore water chemistry, fluid flow, mineralogical partitioning, depositional environment, tectonic setting, time, depth of burial and time of uplift, geothermal gradient and subsurface pressure [2, 3]. Therefore, reconstruction of the diagenetic history of authigenic minerals in sandstone and fine-grained sediments is vital in understanding porosity and permeability to predict the reservoir characteristics of sandstones. The types of minerals formed during sandstones and other clastics diagenesis have direct effect on reservoir characteristics. Mechanically infiltrated clays, authigenic clay minerals, feldspar overgrowths, quartz overgrowths, carbonates and hematite cements have direct control on the reservoir characteristics of the studied sandstone and interbedded fine-grained clastics. The study is needed to understand the abundance and the distribution of diagenetic minerals in sandstones and fine-grained sediments. The main objective of this paper is to study different types of authigenic minerals in different depositional environments and understand their effects on reservoir characteristic in sandstones and fine-grained sediments.

*Corresponding author. E-mail: wolela_am@yahoo.com

Fluviatile and playa sediments (red sandstones, siltstones and mudstones) experienced red-bed diagenesis, whereas the lacustrine sediments (grey mudstones, sandstones and black shales) experienced diagenesis typical of marine mudstones and sandstones [4-7]. The type of mineralized pore water released from the fine-grained sediments has a significant influence on the trends of sandstone diagenesis. Mechanically compacted mudstones, siltstones and shales expelled large volume of mineralized pore water, which might migrated into the sandstone-rich section [8-12].

Based on textural relationships, fluid inclusions, burial and thermal histories and mineral-filled pore spaces, the following paragenetic sequences are reconstructed for the fluvial (subaerially-exposed) sandstones in the Hartford Basin: (1) mechanically infiltrated clay, (2) concretionary calcite, (3) mechanical compaction, (4) grain dissolution, (5) grain coating, (6) feldspar overgrowths, (7) quartz overgrowths, (8) basalt eruption, (9) carbonate cementation, (10) cement and unstable grain dissolution, (11) kaolinite precipitation, (12) hematite cementation, (13) illite cementation, (14) chlorite cementation, (15) authigenesis of euhedral quartz, and (16) hydrocarbon migration; pyrite and apatite precipitation [1, 7, 12].

Lacustrine (subaqueous) sandstones exhibit a different paragenetic sequence in the Hartford Basin: (1) pyrite precipitation, (2) concretionary dolomite, (3) grain dissolution, (4) grain coating clays, (5) feldspar overgrowths, (6) quartz overgrowths, (7) basalt eruption, (8) carbonate cementation, (9) mechanical compaction, (10) cements and unstable grain dissolution, (11) smectite-chlorite, (12) illite cementation, (13) chlorite cementation, (14) authigenesis of euhedral crystals of quartz, and (15) hydrocarbon migration; pyrite and apatite precipitation [7].

Conventional petrographic microscopy, scanning electron microscopy, and electron microprobe can provide information about authigenic minerals in sandstones and fine-grained sediments. Scanning electron microscope (SEM) studies provide information to identify and differentiate authigenic minerals. SEM also provides essential information about the paragenetic sequence of the authigenic minerals. Back-scattered probe analyses gives a significant amount of information about the distribution, abundance and the textural relationship of the authigenic minerals, and also help to differentiate (i) authigenic albite from detrital plagioclase, (ii) authigenic K-feldspar from detrital K-feldspar.

EXPERIMENTAL

In order to understand the abundance of authigenic minerals, integrated studies were carried out on conventional petrographic microscope, electron microprobe (EMP) and scanning electron microscope (SEM). The diagenetic sequences for the sandstones and other fine-grained clastics were reconstructed from conventional petrographic microscopy, scanning electron microscopy and microprobe studies. The paragenetic sequences are reconstructed based on the textural relationship of the authigenic minerals, burial history and fluid inclusions studies. Resin-impregnated thin sections were examined using conventional petrographic microscope, and their modal composition evaluated by counting 300 points.

Unpolished gold-coated chip samples were examined under a JEOL 6400 scanning electron microscope equipped with energy dispersive X-ray analysis (EDX) system with accelerating voltage 10-15 kV, to identify morphology of authigenic minerals, mineral composition and their textural relationships.

Polished carbon-coated chips and thin sections were examined under a JEOL 733 superprobe with an accelerating voltage of 15 kV, to identify the mineralogical composition, textural relationships and zoning in authigenic minerals. A ZAF software programme was used to calculate weight percentage of oxides in each spot analysis. The textural and stratigraphic position of the authigenic minerals plus weight percentage oxide calculations data allowed to

compare the diagenetic trends between sandstones and interbedded siltstones, mudstones and shales.

Fluid inclusion microthermometric measurements were conducted on a petrographic microscope equipped with a Linkam THM 600 microthermometric stage linked with a CS 196 cooling system. A Pr 600 temperature controller was mounted on a Nikon OPTIPHOT2. POL microscope. Imaging was accomplished with a TMC 516 color CCD camera and Hitachi high-resolution monitor with superlong distance lenses of 40x and 60x. The heating-freezing stage was calibrated from -160 to 300 °C. Both sides of polished slices and quartz crystals were examined.

Background geology of the Hartford Basin

The Hartford basin is a half-graben about 150 km long and up to 30 km across [13]. The basin is developed by crustal extension associated with the breaking up of Pangea and the opening of the Atlantic Ocean [14-16]. The basin is in-filled with 4500-5000 m thick clastic sediments including alluvial fans, fluvialite, playa red beds, lacustrine grey and black strata, and extrusive tholeiitic basalts [1, 7, 17-19; Figures 1 and 2].

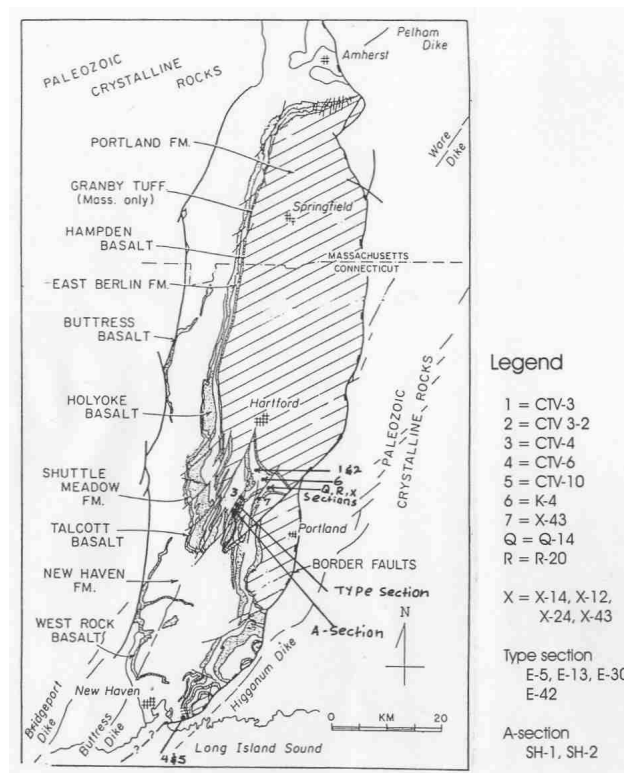


Figure 1. Geological map of the Hartford Basin (after Hubert *et al.* [18]) and sample location map of studied areas in the Hartford Basin.

During initial subsidence in the Upper Triassic, rivers flowed from both sides of the Hartford Basin deposited the New Haven Arkose. The 2 km thick alluvial fan and fluvial red

bed-dominated New Haven Arkose was deposited when the rate of sedimentation exceeded the rate of basin subsidence [18]. Fluvatile, lacustrine and playa-dominated Shuttle Meadow and the East Berlin formations were deposited when the subsidence rate increased to exceed the rate of sedimentation [18].

The 65 m thick Talcot Basalt separated the New Haven Arkose from the Shuttle Meadow formation. The Talcot Basalt dated to be 187 + 10 Ma [20]. Sedimentation returned in the basin after the Talcot Basalt eruption to deposit 150 m thick fluvatile, lacustrine and playa dominated Shuttle Meadow formation [19 and 21].

The 100 m thick Holyoke Basalt separated the Shuttle Meadow formation and East Berlin formation. Sedimentation continued in the basin to deposit the East Berlin formation after the Holyoke Basalt eruption. Gierlowski-Kordesch and Rust [1] classified the East Berlin formation into eight major facies. These include: trough cross-stratified sandstone (St), ripple cross-laminated siltstone (Fr), horizontally stratified sandstone (Sh), interbedded sandstones and mudrocks (Sf), black shale (Fl₁), Stratified mudstones (Fl₂), disrupted shale (Fl₃), and disrupted mudstone (Fm).

The 60 m thick Hampden Basalt eruption interrupted sedimentation of the East Berlin formation. The Hampden Basalt found between the East Berlin formation and the 2 km thick alluvial fan and fluvatile-dominated Portland Formations. The NE-SW trending normal faults cut the basin-fill through the Portland Formation, so that the last movements on them post-dated sedimentation [22, 23].

Era	Period	Formation	Lithology	Maximum Thickness in (m)	Lithology and environment	Hydrocarbon plays
MESOZOIC	Jurassic	Portlandian		2000	Alluvial fan and fluvatile sandy conglomerate, sandstone and siltstone	Reservoir
		Hampden Basalt		60		Seal
		East Berlin		170	Fluvatile, lacustrine and playa sediments	Reservoir, source and seal
		Holyoke Basalt		100		Source
		Shuttle Meadow		150	Fluvatile, lacustrine and playa sediments	Reservoir, source and seal
		Talcot Basalt		65		Seal
	Triassic	New Haven Arkose		2000	Alluvial fan and fluvatile sandy conglomerate, sandstone and siltstone	Reservoir
PRECAMBRIAN		Basement rocks				

Figure 2. Chrono-lithostratigraphic section, depositional environments and hydrocarbon plays of the Hartford Basin.

RESULTS AND DISCUSSION

Diagenetic minerals

Based on conventional petrographic microscope, scanning electron microscope, microprobe microscope, burial history and fluid inclusions the following paragenetic sequences were established from the textural, stratigraphic relationships and fluid inclusion studies of authigenic minerals in sandstone, siltstone and mudstone. The distribution of authigenic minerals in the sandy, silty, muddy and shaly facies in fluvial, playa and lacustrine environments are given in Figures 3-5 and Tables 1, 8-10.

Mechanically infiltrated clays. Mechanically infiltrated clay is widely observed in the studied sediments, and considered to be the earliest facies-related minerals. Mechanical infiltrated clays are found in fluvial sediments, and dominated by smectite and illite-smectite (Figure 7f). SEM studies confirmed the presence of cutans around the detrital framework grains. In places, the primary porosity in the sandy, silty and muddy facies is highly reduced by infiltrated clay. In late-stage diagenesis, mechanically infiltrated clay transformed to authigenic clay minerals (illite and chlorite). Rock with abundant infiltrated clay had a restricted diagenetic evolution. Mechanically infiltrated clay is introduced with meteoric water in the depositional environments [24, 25]. The non-crystalline form indicates their detrital origin.

Authigenesis of concretionary calcite. This is one of the earliest facies-related minerals in the fluvial and playa mudstone, siltstone and sandstone facies. Concretions were precipitated in the intergranular pore spaces by pedogenic processes. The concretions are unevenly distributed in the sandy, silty and muddy facies. Concretions are more abundantly distributed in the sandy facies comparing to the silty and muddy facies (Table 5). Calcrete develop in poorly drained areas in semi-arid to arid environments [26, 27].

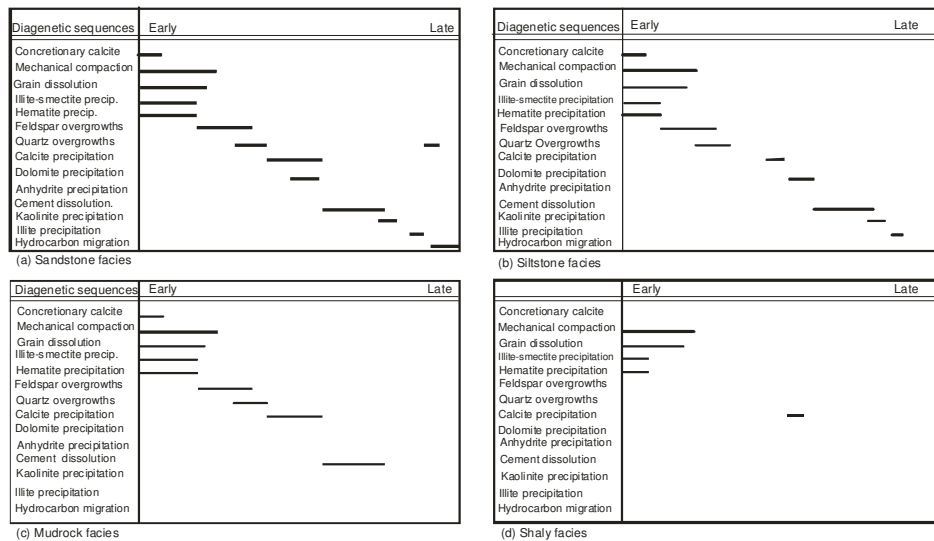


Figure 3. Diagenetic sequences of playa and fluvial sandstones and the interbedded silty, muddy and shaly facies.

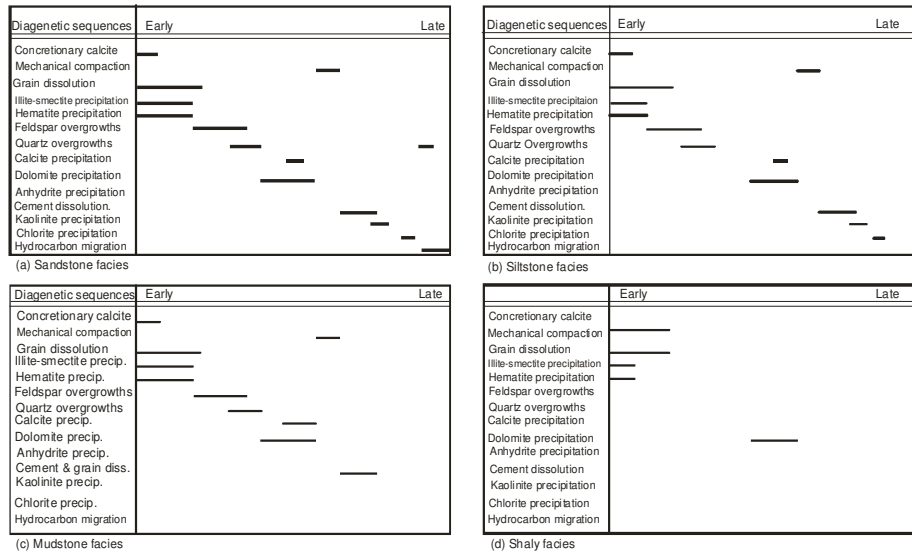
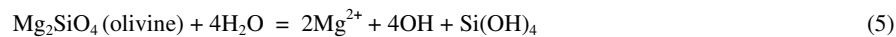
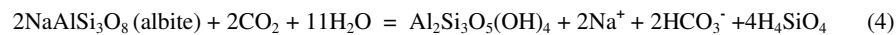
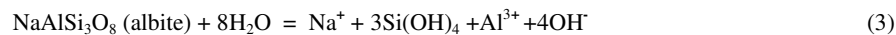
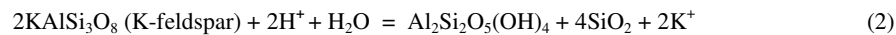
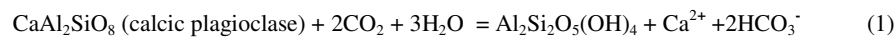


Figure 4. Diagenetic sequences of lacustrine sandstones and the interbedded silty, muddy and shaly facies.

Dissolution of unstable minerals. Carbonic acid formed when meteoric water interacts with CO_2 in the air. Dissolution of unstable minerals is a continuous process during diagenesis. Dissolution of unstable minerals by acidic meteoric pore water is the possible driving force for the precipitation of authigenic minerals in the diagenetic environments [6, 28, 29]. In rift basins, gravity-derived meteoric water flow can penetrate at least several kilometres into the sedimentary basin. Percolation of acidic pore water in the diagenetic environment facilitated dissolution of feldspars and ferromagnesian minerals and released ions of potassium, sodium, aluminium, silicon, calcium, magnesium and iron. Meteoric water plays major role in transport of dissolved ions from areas of high concentration to areas of low concentration.

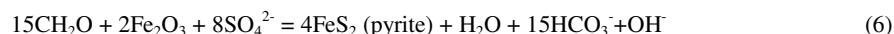


Mechanical compaction. Mechanical compaction took place at early stage of diagenesis in the fluvial and playa sandy, silty and muddy facies. Mechanical compaction in the fluvial and playa fine-grained sediments might have introduced mineralized pore water from the muddy and silty facies into the sandy facies at an early stage of diagenesis. Carbonate and albite cements extensively cemented the lacustrine mudstones, siltstones and sandstones indicating that cementation took place prior to mechanical compaction. Mechanically compacted siltstones, mudstones and shales expelled large volume of mineralized pore water, which migrated into sandstone-rich section in the basin.

Table 1. Diagenetic sequences of fluvatile and lacustrine sediments, East Berlin formation.

Fluviatile sediments	Lacustrine sediments	Zone
(1) Influx of gravity-driven acidic meteoric, water initiated dissolution of unstable, grains and provided ions of potassium, sodium, aluminium, calcium, magnesium and iron	(1) Influx of gravity-driven acidic meteoric, water initiated dissolution of unstable, grains and provided ions of potassium, sodium, aluminium, calcium, magnesium and iron	
(2) Precipitation of concretion	(2) Precipitation of concretion	
(3) Mechanical compaction	(3) Precipitation of pyrite	Sulphate reducing zone
(4) Precipitation of grain-coating clays	(4) Precipitation of grain-coating clays	
(5) Feldspar overgrowths	(5) Feldspar overgrowth	
(6) Quartz overgrowths	(6) Quartz overgrowths	
(7) Carbonate precipitation	(7) Carbonate precipitation	Fermentation zone
(8) Mature source rocks, and clay minerals transformation released carbon dioxide and react with water to form acidic pore water	(8) Mechanical compaction	
(9) Dissolution of carbonate by acidic pore water	(9) Mature source rocks, clay minerals transformation released CO ₂ and react with water to form acidic pore water	Decarboxylation zone
(10) Precipitation of pore-filling clays	(10) Dissolution of carbonate cements by acidic pore water	
(11) Oil emplacement in fluvatile sandstone	(11) Precipitation of pore-filling clays	
	(12) Oil emplacement and precipitation of pyrite and apatite	Oil generation zone

Pyrite precipitation. SEM and probe studies confirmed the presence of pyrite crystals (Figure 6a). Pyrite crystals range from 1 to 30 µm in the silty and muddy facies and 10 to 100 µm in the sandy facies. Pyrite is the earliest diagenetic mineral in the lacustrine grey mudstone, siltstone and sandstone facies. Pyrite is found only in the lacustrine sediments, and formed at an early stage of diagenesis in the sulphate-reducing zone below the sediment-water interface [5]. Pyrite crystals mainly occur as disseminated patches. However, pyrite crystals are also found along the bedding planes and lamination. The presence of pyrite is an indicator of anoxic environment. Late-stage diagenetic pyrite crystals are identified in the sandy facies associated with bitumen. Minor amounts of apatite are also identified in bitumen-bearing sandstones.



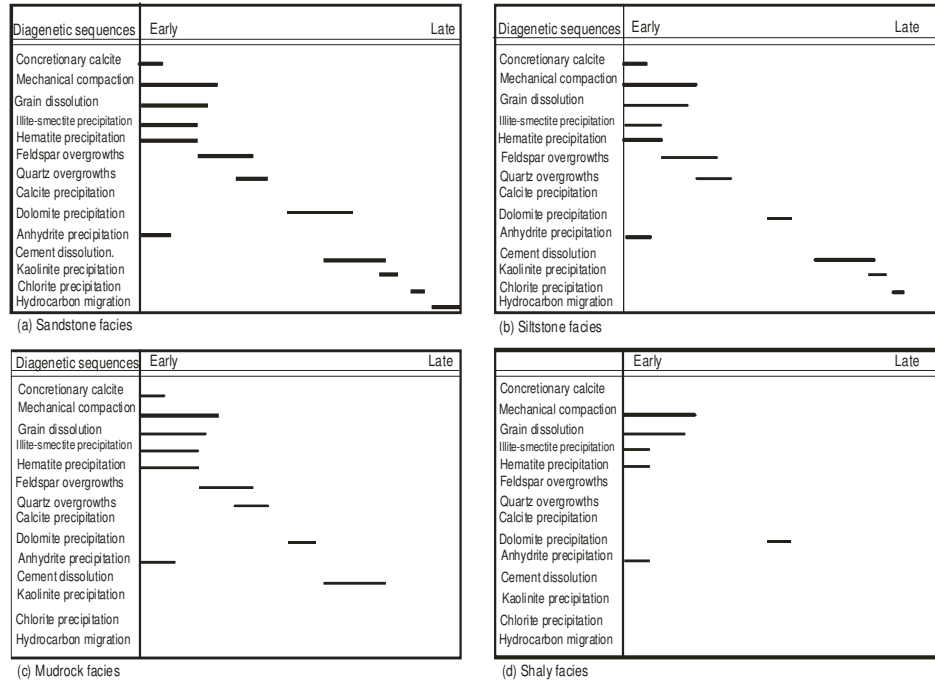


Figure 5. Diagenetic sequences of playa sandstones and the interbedded silty, muddy and shaly facies.

Authigenesis of clay minerals. Clay minerals exist as grain-coating, pore-lining and pore-filling cements (Figure 6d and f). Grain-coating clays are one of the earliest authigenic minerals in the studied fluvatile, playa and lacustrine mudstone, siltstone and sandstone facies.

SEM studies indicate the presence of smectite-chlorite in the playa sandy, muddy and silty facies. Illite is the predominant clay mineral in fluvial sequences (Figure 6d), whereas the lacustrine sandstones, siltstones and mudstones are dominated by minor amounts of box-work illite-smectite and box-work to rosette smectite-chlorite (Figure 6d). Microprobe analyses revealed the presence of potassium, magnesium, calcium, silicon, aluminium and iron, indicating illite-smectite and smectite-chlorite.

The lower abundance of authigenic clay minerals in the lacustrine sediments possibly indicates that the saline pore waters condition were not suitable for the authigenesis of clay minerals or related to albitization i.e. metasomatism in the expense of clay minerals and quartz [30].

Authigenesis of feldspar. Petrographic microscopy, SEM and probe studies confirmed the presence of feldspar overgrowths and euhedral crystals in the muddy, silty and sandy facies. Albite overgrowths are the predominant feldspar types. Authigenesis of feldspar overgrowths was commenced in the mid stage of diagenesis (Figures 3-5). The overgrowths range from 5 to 15 μ m in the sandy facies, and 1 to 8 μ m in the muddy and silty facies (Figures 6b and c; 7a, b and c). Microprobe weight percentage calculations on authigenic crystals of albite in the playa muddy facies revealed average compositions of 69.48% SiO₂, 20.77% Al₂O₃ and 9.74% Na₂O, whereas authigenic crystals of albite in the playa sandy facies revealed average composition of

69.82% SiO_2 , 20.88% Al_2O_3 and 9.64% Na_2O with minor impurities of CaO (0.395-3.2%) (Table 2). Microprobe weight percentage calculations of albite crystals in the lacustrine sandstones revealed average compositions of 68.74% SiO_2 , 20.82% Al_2O_3 and 10.43% Na_2O (Table 2).

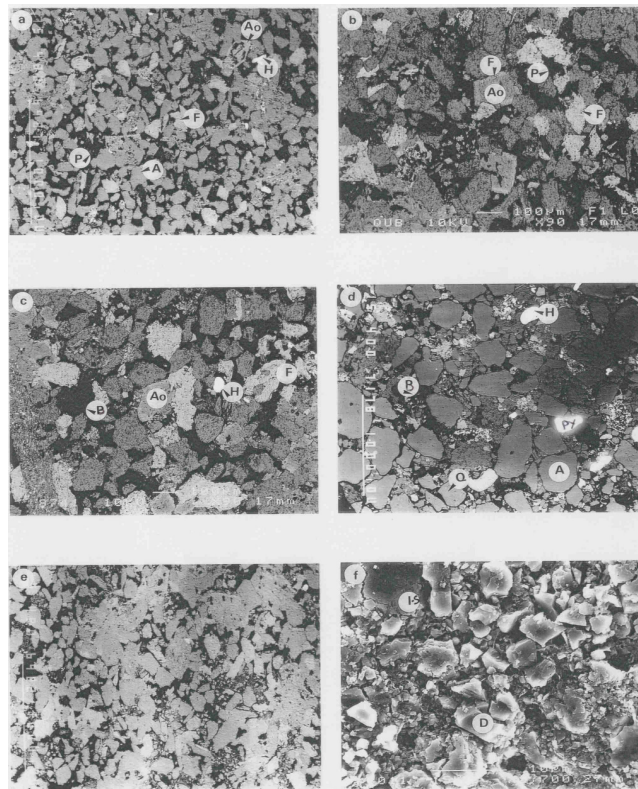


Figure 6. (a) Back-scattered photomicrograph showing pyrite crystals (Py) associated with feldspar grains in shallow lake sandstone (scale bar 10 microns). (b) Back-scattered photomicrograph showing feldspar grains (F), authigenic albite (Ao) and hematite/illite (H/I) in alluvial siltstone sample (scale bar 1000 microns). (c) SEM photomicrograph showing authigenic K-feldspar (Fo) in ripple cross-laminated alluvial siltstone (scale bar 10 microns). (d) SEM photomicrograph showing pore-filling albite crystals (Ao) and illite (I) in stratified mudstone sample (scale bar 1 micron). (e) SEM photomicrograph showing pore-filling calcite (C) in ripple cross-laminated alluvial fan siltstone (scale bar 10 microns). (f) SEM photomicrograph showing pore-filling dolomite (D) and chlorite (Ch) in black shale sample (scale bar 1 micron).

Microprobe weight percentage calculations of authigenic K-feldspar crystals in the lacustrine muddy facies revealed average compositions of 63.96% SiO_2 , 19.4% Al_2O_3 and 16.37% K_2O . Whereas K-feldspar crystals in the sandy facies revealed average compositions of 64.03% SiO_2 , 19.44% Al_2O_3 and 16.53% K_2O with minor impurities of Na_2O (0-1.02%) (Table 5). Authigenic K-feldspar or albite overgrowths are absent in the shaly facies.

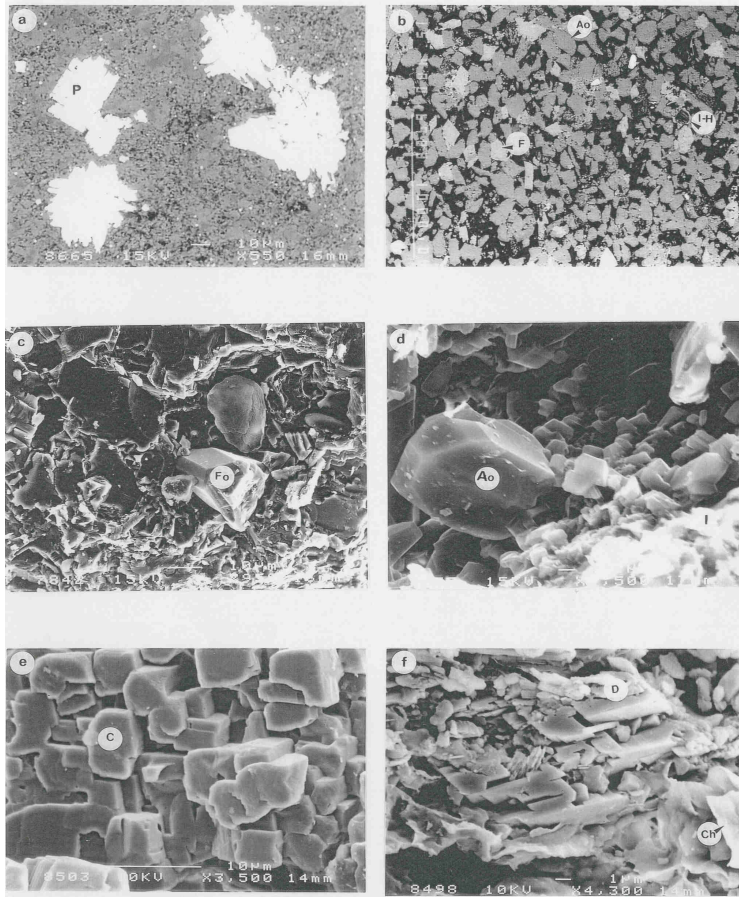


Figure 7. (a) Back-scattered photomicrograph showing albite grain (A), K-feldspar grains (F), albite overgrowths (Ao), porosity (P) and hematite (H) in alluvial/sandflat siltstone to interdedded sandstone sample (scale bar 1000 microns). (b) Back-scattered photomicrograph showing albitization (Ao) of K-feldspar (F) and pore space (P) in alluvial/sandflat trough cross-bedded sandstone sample (scale bar 100 microns). (c) Back-scattered photomicrograph showing K-feldspar (F) albite overgrowths (Ao), Hematite (H) and porosity (P) in alluvial/sandflat trough cross-bedded sandstone sample (scale bar 100 micron). (d) Back-scattered photomicrograph showing disintegration of iron-bearing grain, quartz (Q), albite (A), hematite (H) and porosity (P) in alluvial plain cross-laminated siltstone to interbedded sandstone and mudstone sample (e) Back-scattered photomicrograph showing distributions of minerals, pore space and remnant floaters in pore spaces in alluvial ripple cross-laminated siltstone sample (scale bar 1000 microns). (f) SEM photomicrograph showing extensive detrital dolomite (D) and detrital illite (I) in offshore lacustrine black shale (scale bar 1000 microns).

Table 2. Microprobe analyses (% composition) of authigenic albite (East Berlin formation).
Ab = albite, Or = orthoclase and An = anorthite.

Sample No	Location	Lithology	SiO ₂	Al ₂ O ₃	CaO	Na ₂ O	Average Ab	Average Or	Average An
E-30	Playa	Sandstone	65.14	23.09	2.47	9.29	99.9		0.1
			69.28	20.56		10.16			
			68.99	20.5		10.51			
			61.26	24.89	2.69	11.16			
			65.49	22.84	3.2	8.47			
			70.28	20.19		9.53			
			69.36	20.08		10.55			
			68.58	20.65		10.77			
			68.26	20.94	0.39	10.41			
Q-14	playa	Mudstone/ siltstone	68.28	20.43		11.29	99.6	0.1	0.3
			69.79	20.44		9.77			
			70.38	21.46		8.16			
E-5	Lacustrine	Sandstone	69.86	20.83		9.31	99.1		0.9
			70.34	20.75		8.91			
			68.99	22.03	0.68	8.31			
			69.69	20.53		9.77			
			69.65	21.06		9.29			
K-4	Fluviatile	Sandstone	70.08	20.79		9.14	98.8	0.4	0.8
			69.76	21.69		8.55			
			68.58	20.68		10.74			
CTV-4	Lacustrine	Sandstone	67.87	20.75		11.38	98	1	1
			68.12	20.77		11.12			
			67.79	20.43		11.78			
			67.56	20.1		12.35			
			67.77	20.66		11.57			
			68.4	20.74		10.86			
			67.76	20.61		11.63			

Intergranular dissolution of unstable grains (feldspar and ferromagnesian) is the main source for the authigenesis of K-feldspar and albite in the playa and lacustrine depositional environments. The abundance of albite cement in the playa and lacustrine sandstones, siltstones and mudstones indicates the abundance of aluminium, silicon and sodium ions in the pore waters. The lower abundance of K-feldspar overgrowths and crystals in the playa and lacustrine sediments might be related to albitization. When K-feldspar reacts with sodium ions, yield albite and released potassium ions [30]. The abundance of albite crystals (Figures 6d, 7b and c) in the sandy facies near the sandstone-siltstone and sandstone-mudstone contacts indicates pore water and mass transfer from the fine-grained sediments into the sandstone facies [10-12]. Feldspar overgrowths abundantly distributed in the sandy facies comparing to silty and muddy facies.

Table 3. Microprobe analyses (% composition) of detrital plagioclase feldspar (East Berlin formation, Hartford Basin). Ab = albite, Or = orthoclase and An = anorthite.

Sample No	Location	Lithology	SiO ₂	Al ₂ O ₃	CaO	Na ₂ O	Average Ab	Average Or	Average An
E-30	Playa	Sandstone	65.076	22.634	3.072	9.827	83.7	1.8	14.5
			63.017	22.563	2.988	10.032			
Q-14	Playa	Mudstone/siltstone	65.255	22.480	3.136	9.895	83.6	1.7	14.7
			65.011	20.440	3.217	9.770			
E-5	Lacustrine	Sandstone	63.695	21.659	2.218	10.55	81.1	9.4	9.5
			63.891	20.750	2.312	9.989			
K-4	Fluviatile	Sandstone	61.631	23.845	4.535	9.387	78.8	0.2	21
			62.213	22.981	4.023	9.125			
CTV-4	Lacustrine	Sandstone	65.145	22.361	2.542	10.251	84	1	15
			65.112	23.001	2.523	10.998			

Table 4. Microprobe analyses (% composition) of authigenic K-feldspar (East Berlin formation, Hartford Basin).

Sample No	Location	Lithology	SiO ₂	Al ₂ O ₃	Na ₂ O	K ₂ O	Average Ab	Average Or	Average An
E-30	Playa	Sandstone	64.23	19.53	0.84	15.4	2.7	97.2	0.1
			64.2	19.64		16.16			
			64.15	19.31		16.54			
			64.25	19.8		15.95			
			64.45	19.07		16.48			
X-12	Lacustrine	Mudstone	64.29	19.71		16	1	99	
			63.29	19.96	1.12	15.64			
K-4	Fluviatile	Sandstone	64.05	19.25	0.8	15.9	0.9	99.1	
			64.28	19.78		15.94			
CTV-4	Lacustrine	Sandstone	64.18	19.49		16.33	0.8	99.2	
			63.94	19.81		16.24			
			63.75	19.36		16.88			
			63.99	18.95	1.02	16.04			

Table 5. Microprobe analyses of (% composition) of detrital K-feldspar (East Berlin formation, Hartford Basin). Ab = albite, Or = orthoclase and An = anorthite.

Sample No	Location	Lithology	SiO ₂	Al ₂ O ₃	Na ₂ O	K ₂ O	Average Ab	Average Or
E-30	Playa	Sandstone	64.066	19.231	0.492	14.975	4.4	95.6
			64.122	19.640	0.349	16.16		
X-12	Lacustrine	Mudstone siltstone	63.965	18.793	0.927	14.288	9	91
			63.006	18.76	0.819	15.001		
K-4	Fluviatile	Sandstone	64.174	18.711	0.688	15.836	6.2	93.8
			64.218	18.178	0.544	15.114		
CTV-4	Lacustrine	Sandstone	62.548	18.754	1.03	15.549	6.9	93.1
			62.762	18.998	1.097	15.56		

Microprobe studies in carbon coated polished sections not allowed to differentiate authigenic albite from detrital plagioclase feldspar, and also authigenic K-feldspar from detrital K-feldspar. However, ternary plot based on pure anorthite (An), pure albite (Ab) and pure

orthoclase (Or) end member showed that authigenic albite plotted near the apices of Ab (Figure 8a), whereas detrital plagioclase plotted away from the Ab apices (Figure 8b).

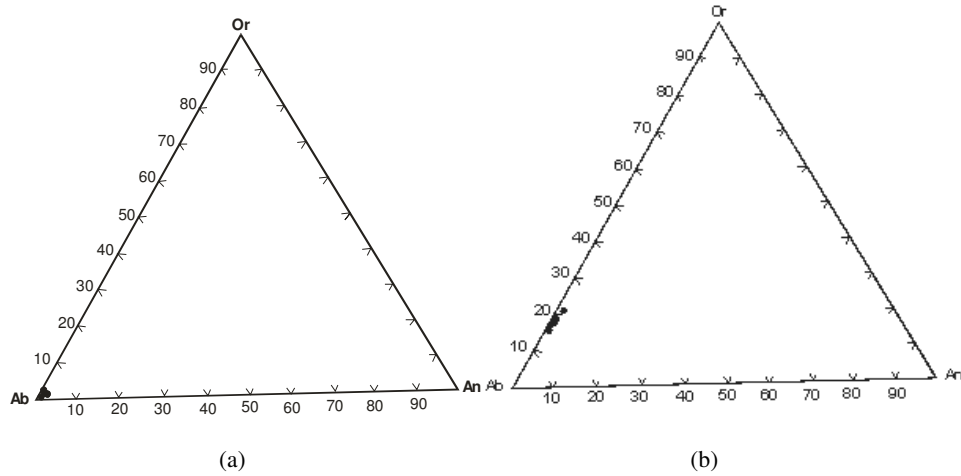


Figure 8. (a) Ternary plot for authigenic K-feldspar based upon anorthite (An), albite (Ab) and orthoclase (Or) end members. (b) Ternary plot for detrital K-feldspar based upon anorthite, albite and orthoclase end members.

Authigenic K-feldspar crystals are plotted near the apices of Or (Figure 9a), whereas the detrital K-feldspar plotted away from the apices of Or (Figure 9b). The distribution of authigenic albite and authigenic K-feldspar near the apices of Ab and Or indicate their authigenic origin. The distribution of the detrital plagioclase feldspar and detrital K-feldspar away from the Ab and Or apices indicated their detrital origin. Microprobe analyses of authigenic K-feldspar and detrital K-feldspar and authigenic albite and detrital plagioclase feldspar are given in Tables 2-5.

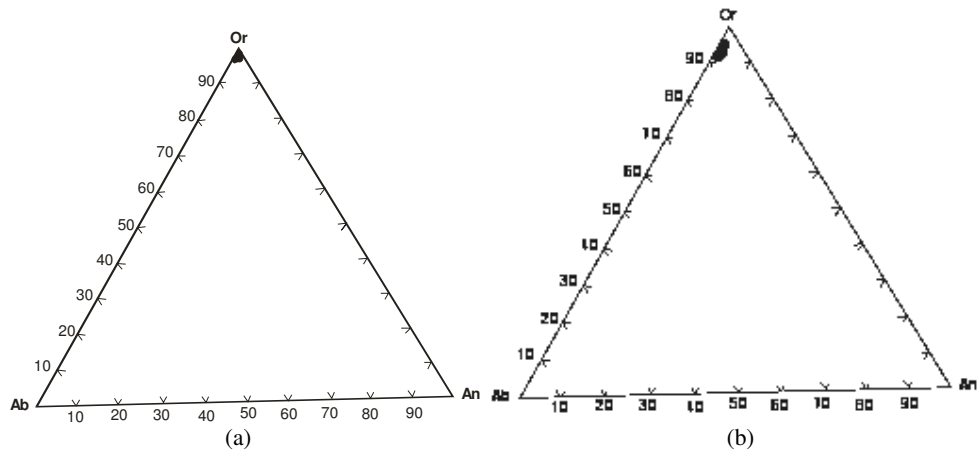


Figure 9. (a) Ternary plot for authigenic albite based upon anorthite, albite and orthoclase end members. (b) Ternary plot for detrital plagioclase based upon anorthite, albite and orthoclase end members.

Authigenesis of quartz. Petrographic microscope and SEM studies revealed the presence of euhedral crystals and overgrowths in the muddy, silty and sandy facies. Quartz overgrowths and crystals are less common compared to authigenic feldspar overgrowths and crystals. The authigenic quartz crystals range from 1 to 5 μm across in the silty and muddy facies, whereas the authigenic quartz crystals in the sandy facies range from 10 μm to 100 μm . The possible sources for quartz authigenesis include: (i) dissolution of unstable framework grains (feldspar and ferromagnesian minerals), and (ii) mass transfer of silicon ions into the pore water from the interbedded fine-grained sediments. Part of the silica budget might have come from the underlying and overlying interbedded fine-grained sediments through compaction and diffusion [12]. In subsiding rift basins, dissolved material moves from areas of high concentration to areas of low concentration. Many workers [12, 31, 32, 33] invoke fine-grained sediments as a source for silica cementation. Quartz overgrowths abundantly distributed in sandy facies comparing to silty and muddy facies.

Circular and elliptical, aqueous and petroleum fluid inclusions in the late stage quartz crystals yielded temperatures of entrapment from 110 to 130 $^{\circ}\text{C}$ (Figure 10). Quartz crystals contain both aqueous and hydrocarbon inclusions indicating that quartz authigenesis continued during oil emplacement.

The possible sources for the silicon ions might be: (1) the dissolution of ferromagnesian minerals, (2) percolation of topography and gravity-driven meteoric silicon-rich pore water, (3) dissolution of feldspar, and (4) pore-water and mass exchange from the interbedded mudrocks, siltstones and shales [7]. Quartz overgrowths start as numerous minute, incipient pyramidal prisms that developed into well-developed crystal faces. Continued merging of faces to develop euhedral crystals indicates that the physicochemical conditions, i.e. pore water super-saturation with silicon ions, pore space and time were adequate [7].

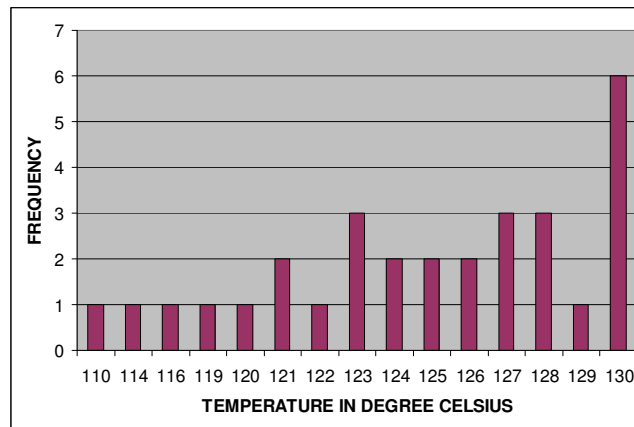


Figure 10. Fluid inclusion data for East Berlin formation.

Carbonate cementation. Carbonate cementation took place in early and late stage diagenesis. The early stage concretionary carbonates (calcrete) are characterized by their non-replacive simple pore-filling nature. Precipitation of iron-rich carbonate in the fermentation zone and iron-poor carbonate precipitation in the sulphate reduction zone is well documented [5].

Table 6. Microprobe analyses (% composition) of dolomite and ferroan dolomite cements (East Berlin formation).

Sample No	Location	Sample type	SiO ₂	Fe ₂ O ₃	CaO	MgO	MnO
E-30	Playa	Sandstone	1.059	8.404	27.68	16.253	
			0.539	11.062	26.94	14.566	
			0.61	12.919	26.661	12.662	
			0.871	10.231	28.172	14.247	
			0.313	8.142	29.671	16.772	
			4.944	31.363	11.501	1.28	
X-14	Lacustrine	Siltstone	0.671	5.742	26.524	18.332	2.708
			1.538	2.538	29.101	15.939	0.699
				3.395	31.742	19.039	0.851
			1.266	2.972	30.454	16.176	0.917
			0.34		32.317	22.37	
			0.342		31.402	21.209	
			0.464		31.354	21.238	
			0.515	31.68	19.829		
X-12	Lacustrine	Mudstone		8.579	24.231	15.946	
				20.306	25.753	16.921	
				19.327	27.955	17.367	
SH-1	Lacustrine	Shale		2.412	27.806	16.764	
			0.888	2.386	27.023	17.253	
			1.947	2.034	26.169	17.56	
			1.022	2.37	26.374	16.503	
			0.86	3.013	28.539	15.22	
			0.498	3.107	28.309	16.544	
			0.727	3.454	27.39	15.851	
	0.369	2.003	28.862	18.315			
SH-2	Lacustrine	Shale		5.196	30.006	16.931	
			4.396	4.59	27.129	15.448	
			0.698	4.217	27.099	16.806	
			0.632	5.791	28.626	16.809	
			1.992	0.783	28.428	16.829	
			0.415	5.274	29.204	15.973	
				0.543	28.883	18.628	
			0.449		28.6	18.013	
		29.287	17.287				
CTV-4	Lacustrine	Sandstone		2.336	27.736	17.071	
				8.44	27.37	15.109	
			0.367	12.557	24.097	10.522	
				12.891	25.352	10.753	
				12.314	25.314	11.227	0.473
				10.742	25.533	12.258	0.758
	9.161	27.156	12.87	0.758			
	1.452	48.057	4.444	0.864			

Table 7. Microprobe analyses (% composition) of calcite cements (East Berlin formation, Hartford Basin).

Sample No	Location	Sample type	SiO ₂	Fe ₂ O ₃	CaO	MgO	MnO
CTV-6	Fluviatile	Sandstone	0.903		50.73	0.476	0.918
			0.825	0.472	50.818		
			0.337		55.301		1.635
			0.217		52.311		
K-4	Fluviatile	Siltstone/ siltstone			57.496		
					59.917		
					57.732		
					58.387		
					56.651		

Late stage replacive carbonate cements extensively cemented the fluviatile, playa and lacustrine sediments. Varieties of carbonate cements (calcite, ferroan calcite, dolomite, ferroan dolomite and ankerite) (Figures 6e and f) occur in the fluviatile, playa and lacustrine sediments. The variation in carbonate cements depends upon the availability of metallic cations, due to the breakdown of various minerals in different diagenetic zones [4]. Dolomite and ferroan dolomite widely distributed in playa and lacustrine sandstones and fine-grained sediment, whereas calcite cement dominated fluviatile sandstone and fine-grained sediments.

The lacustrine mudstones, siltstones and sandstones extensively cemented by dolomite and ferroan dolomite. Calcite cements are abundantly distributed in the fluviatile sediments (Figure 6e). Volumetrically, dolomite is the most extensively distributed carbonate cement in the lacustrine and playa silty, muddy and sandy facies. It is characterized by both euhedral and microcrystalline forms. The abundance of dolomite cement in the lacustrine and playa settings reflects the concentration of magnesium and/or contraction of the saline lake through evaporation to elevate the Mg/Ca ratios.

Mechanical compaction of fine-grained sediments might have released ions into the sandy facies for the authigenesis of carbonate cements. The abundance of carbonate crystals in the sandy facies near the sandstone-mudstone and sandstone-siltstone contacts (Figures 6e and f) indicates mass transfer (pore water and ions) from the fine-grained sediments into the sand-rich section of the basin. The silty and muddy facies are dominated by detrital carbonate rock fragments (6f). XRF results indicate that the upper grey mudstones have MgO contents up to 7.02%. The black shales, which are interbedded between the upper grey laminated mudstones and lower laminated grey mudstones contain MgO (13.69%), whereas the lower grey mudstones contain up to 3.97% [34]. The grey mudstones and black shales that are interbedded within the sandstone facies are possible a source of the carbonate cements in the sandy facies. The most important sources of ions for the authigenesis of carbonate cements in the fluviatile, playa and lacustrine settings included: (i) interstitial dissolution of unstable minerals, (ii) mass transfer of ions in pore waters from interbedded siltstones, mudstones and shales, and (iii) calcrete (CaCO₃) in fluviatile flood plain sediments most likely source of calcite cementation in the sandy facies near the calcrete horizons.

Microprobe analyses of dolomite in the lacustrine muddy and silty facies revealed an average Mg/Ca ratio of 0.649, whilst the dolomite cement in the sandy facies have an average Mg/Ca ratio of 0.676. Microprobe analyses on ferroan dolomite and ankerite cement in the fine-grained lacustrine sediments (siltstones and mudstones) have average ratio of Fe/Ca 0.207 and Mg/Ca ratio of 0.561, whilst the ferroan dolomite cements in the sandy facies revealed in average Fe/Ca ratio of 0.303 and Mg/Ca ratio of 0.360. Microprobe analyses on ferroan dolomite in the playa sandstone revealed an average Fe/Ca ratio of 0.298, Mg/Ca ratio of 0.502 and Mn/Ca ratio of 0.010. Microprobe analyses on ankerite cement in the playa sandstones

revealed an average Fe/Ca ratio of 0.410, Mg/Ca ratio of 0.479 and Mn/Ca ratio of 0.029. Microprobe analyses of carbonate cements are given in Tables 6 and 7.

Table 8. Detrital and authigenic minerals abundance in fluvatile sediments, East Berlin formation.

Detrital minerals	Abundance	Detrital minerals	Abundance	Detrital minerals	Abundance
Quartz	xx	Quartz	xx	Quartz	xx
Feldspar	xxxx	Feldspar	xxxx	Feldspar	xxx
Rock fragments	x	Rock fragments	x	Rock fragments	x
Detrital clay	xx	Detrital clay	xx	Detrital clay	xxx
Micas	x	Micas	xx	Micas	xx
Heavy minerals	x	Heavy minerals	x	Heavy minerals	x

Sandstone		Siltstone		Mudstone	
Authigenic minerals	Abundance	Authigenic minerals	Abundance	Authigenic minerals	Abundance
Concretion	xx	Concretion	x	Concretion	x
Illite-smectite	xx	Illite-smectite	xx	Illite-smectite	x
Feldspar overgrowths	xxxx	Feldspar overgrowths	xxx	Feldspar overgrowths	xx
Quartz overgrowths	xxx	Quartz overgrowths	xx	Quartz overgrowths	x
Caclite	xx	Caclite	xx	Caclite	xx
Kaolinite	xx	Kaolinite	x	Kaolinite	x
Hematite	xx	Hematite	xx	Hematite	x
Illite	xx	Illite	x	Illite	x

Detrital minerals	Abundance	Authigenic minerals	Abundance
Feldspar	xxx	Concretion	
Rock fragments	xx	Illite-smectite	x
Detrital clay	xxxx	Feldspar overgrowths	
Micas	xx	Quartz overgrowths	
Heavy minerals	x	Caclite	x
Shale		Kaolinite	
		Hematite	x
		Illite	x
		Shale	

Key: xxxx = major, xxx = moderate, xx = minor, x = very minor.

Table 9. Detrital and authigenic minerals abundance in lacustrine sediments, East Berlin formation.

Detrital minerals	Abundance	Detrital minerals	Abundance	Detrital minerals	Abundance
Quartz	xx	Quartz	xx	Quartz	xx
Feldspar	xxxx	Feldspar	xx	Feldspar	x
Rock fragments	x	Rock fragments	x	Rock fragments	x
Detrital clay	xx	Detrital clay	xx	Detrital clay	xx
Micas	x	Micas	x	Micas	xx
Heavy minerals	x	Heavy minerals	x	Heavy minerals	x
Sandstone		Siltstone		Mudstone	

Authigenic minerals	Abundance	Authigenic minerals	Abundance	Authigenic minerals	Abundance
Pyrite	xx	Pyrite	x	Pyrite	x
Illite-smectite	xxx	Illite-smectite	xx	Illite-smectite	x
Feldspar overgrowths	xxxx	Feldspar overgrowths	xx	Feldspar overgrowths	x
Quartz overgrowths	xxx	Quartz overgrowths	xx	Quartz overgrowths	x
Caclite	x	Caclite	x	Caclite	x
Dolomite	xxxx	Dolomite	xxx	Dolomite	xxx
Kaolinite	xx	Kaolinite	x	Kaolinite	
Smectit-chlorite	xx	Smectit-chlorite	x	Smectit-chlorite	x
Hematite	xx	Hematite	xx	Hematite	x
Chlorite	xx	Chlorite	x	Chlorite	x
Sandstone		Siltstone		Mudstone	

Detrital minerals	Abundance	Authigenic minerals	Abundance
Quartz	x		
Feldspar	x	Pyrite	
Rock fragments	x	Illite-smectite	x
Detrital clay	xxxx	Feldspar overgrowths	
Micas	xx	Quartz overgrowths	
Heavy minerals	x	Caclite	x
Shale		Dolomite	x
		Kaolinite	
		Smectit-chlorite	
		Hematite	x
		Chlorite	

Key: xxxx = major, xxx = moderate, xx = minor, x = very minor.

Table 10. Detrital and authigenic minerals abundance in playa sediments, East Berlin formation.

Detrital minerals	Abundance	Detrital minerals	Abundance	Detrital minerals	Abundance
Quartz	xx	Quartz	x	Quartz	x
Feldspar	xxxx	Feldspar	xxx	Feldspar	xx
Rock fragments	x	Rock fragments	x	Rock fragments	x
Detrital clay	xx	Detrital clay	xx	Detrital clay	xxx
Micas	x	Micas	xx	Micas	xx
Heavy minerals	x	Heavy minerals	x	Heavy minerals	x
Sandstone		Siltstone		Mudstone	
Authigenic minerals	Abundance	Authigenic minerals	Abundance	Authigenic minerals	Abundance
Concretion	xx	Concretion	x	Concretion	x
Illite-smectite	xx	Illite-smectite	xx	Illite-smectite	x
Feldspar overgrowths	xxxx	Feldspar overgrowths	xxx	Feldspar overgrowths	xx
Quartz overgrowths	xxx	Quartz overgrowths	xx	Quartz overgrowths	x
Kaolinite	xx	Kaolinite	x	Kaolinite	x
Hematite	xx	Hematite	xx	Hematite	x
Illite	xx	Illite	x	Illite	x
Sandstone		Siltstone		Mudstone	

Detrital minerals	Abundance	Authigenic minerals	Abundance
Feldspar	x	Concretion	
Rock fragments	x	Illite-smectite	x
Detrital clay	xxxx	Feldspar overgrowths	
Micas	xx	Quartz overgrowths	
Heavy minerals	x	Kaolinite	
Shale		Hematite	x
		Illite	x

Key: xxxx = major, xxx = moderate, xx = minor, x = very minor.

Reservoir properties

Depositional environment, pore-water chemistry, diagenetic processes, burial and thermal history of the basin governed the porosity evolution of the studied sandstone and other clastic sediments. The fluvial and lacustrine sandstones are more porous than the fine-grained clastic sediments. Carbonic acid is formed when rain water reacts with carbon dioxide in the air. Secondary porosity was generated due to the percolation of gravity-driven acidic meteoric water during early diagenesis. Circulation of meteoric water in the diagenetic environment facilitated the dissolution of unstable grains to generate secondary porosity. In rift basins, gravity-driven acidic meteoric water flow can penetrate at least several kilometers in the sedimentary basin. In late diagenesis, mature source rocks and clay minerals transformation released CO₂, which

facilitated the entry of acidic pore-water into the diagenetic environment to dissolve the carbonate cements and unstable framework grains to generate secondary porosity (Figure 7a and b). In the East Berlin formation, secondary porosity was generated before oil migration, as evidenced by the presence of bitumen in some of the secondary porosity (Figure 7c and d).

Mechanical compaction, grain-coatings and pore-lining and pore-filling (clay minerals, feldspar overgrowths, quartz overgrowths and carbonate cements) are major factors in reducing intergranular porosity. The porosity in the fine-grained clastic sediments is highly diminished by mechanical compaction and cementation. Some of the studied interbedded siltstones and mudstones in the East Berlin formation exhibited fair to good porosity up to 20% (Figures 6b, 7a and f), whereas such pores have poor interconnectedness. The pore throats of such rocks are too small for oil to pass due to high capillary pressure [35]. Permeability is controlled by many factors such as effective porosity of the rock, geometry of pores, tortuosity, size of the throat between the pores, the capillary force between the rock and pressure gradient and fluid flow [36]. The sandy facies is the most porous and permeable potential reservoir for oil and gas, whereas the muddy and silty facies are possible gas reservoir.

The presence of interbedded siltstones, mudstones and shales in the sandstone facies accounts for porosity loss in sandstone facies. The sandy facies near sandstone-siltstone and sandstone-mudstone contacts exhibited porosity loss due to extensive quartz crystals precipitation.

Interpretation

The diagenetic processes that took place in the sandy facies also took place in the muddy and silty facies. Grain-coating clay/hematite, pore-filling and pore-lining clays, quartz overgrowths, feldspar overgrowths, carbonate cements are observed in the sandstone, siltstone and mudstone facies. The distribution of authigenic minerals varies in the sandy, silty and muddy facies. This might be related to distribution of permeability and the supersaturation of the pore water with respect to silicon, aluminium, potassium, sodium, calcium, magnesium and iron ions. The abundance of authigenic minerals in decreasing order include: sandstone > siltstone > mudstone > shale. The abundance of authigenic minerals in the sandstone facies might be related to the distribution of permeability, which might acted as a conduit for formation water circulation. Except minor amounts of authigenic illite-smectite and illite the shaly facies is dominated by detrital carbonate, quartz and feldspar grains.

The studied fluvial and playa sandstones and fine-grained sediments followed red bed diagenesis, whereas the lacustrine sediments followed marine diagenesis [7]. Syn-depositional minerals variations were encountered in the depositional environments. At early stage of diagenesis, the fluvial sandstones and fine-grained sediments are dominated by mechanically infiltrated clays, pedogenic mud aggregates and concretionary calcite. The playa sandstones and fine-grained sediment is dominated by concretionary dolomite, whereas the lacustrine sediments are dominated by pyrite crystals.

There are variations in clay mineralogy. Mechanically infiltrated clays are found in the fluvial sandstones and fine-grained sediments, and dominated by illite and illite-smectite. In some sandstone, siltstone and mudstone samples, primary porosity is highly reduced by infiltrated clay. In places, the authigenesis of carbonate cements, quartz and feldspar overgrowths and generation of secondary porosity retarded by the abundance distribution of mechanically infiltrated clays [7, 18]. The authigenic clay minerals in the East Berlin formation are dominated by illite in the fluvial sequence and smectite-chlorite, illite-smectite in the lacustrine sandstones, siltstones and mudstones. In places, mixed-layers (illite-smectite and smectite-chlorite) in the East Berlin formation have the most marked effect on the reservoir properties, reducing porosity to zero.

There are variations in carbonate cements in the East Berlin formation. Dolomite, ferroan dolomite and ankerite were restricted to the lacustrine sandstones, siltstones and mudstones indicating that saline alkaline conditions were suitable for precipitation these minerals [7]. Abundance of calcite found in the fluvial sandstones possibly indicates open drainage. Calcite cementation in the fluvial depositions is possibly due to abundance distribution of concretionary calcite, and the dissolution of concretionary calcite provided ions for the authigenesis of calcite. The dissolution of carbonate cements in the late stage of diagenesis produced secondary porosity, and improved the permeability and other reservoir properties of the studied sediments.

Possible sources for the dolomite, ferroan dolomite and ankerite cements are: (i) percolation of mineralized water from leaching of dolomite marble from the source area [18], (ii) concentration of Mg^{2+} in a closed-basin alkaline hard water lake, (iii) alteration and/or dissolution of detrital pyroxene, amphibole, biotite, magnetite, and ilmenite, (iv) dissolution of oligoclase-rich plagioclase by interstitial pore water, (v) contraction of the saline lake increased concentration of magnesium, and (vi) fluid and mass exchange from the interbedded mudrocks, siltstones, and shales [7, 12, 18, 19]. Microprobe analysis in the interbedded mudrocks confirmed the presence of extensive dolomite cements [7].

CONCLUSIONS

(1) Reconstruction of the paragenetic sequences in the studied sandstone and the interbedded mudstones and siltstones revealed the same authigenic minerals association. Paragenetic sequences in fluvial and playa mudstones, siltstones and sandstones in the East Berlin formation indicated red bed diagenesis, whilst the diagenetic trend for the lacustrine mudstones, siltstones and sandstones is equivalent to that of marine clastic diagenesis. (2) The diagenetic processes that took place in the sandy facies also took place in the muddy and silty facies. Grain-coating clay/hematite, pore-filling and pore-lining clays, quartz overgrowths, feldspar overgrowths, carbonate cements are observed in the sandstone, siltstone and mudstone facies. The distribution of authigenic minerals varies in the sandy, silty and muddy facies. This might be related to distribution of permeability and the supersaturation of the pore water with respect to silicon, aluminium, potassium, sodium, calcium, magnesium and iron ions. The abundance of authigenic minerals in decreasing order include: sandstone > siltstone > mudstone > shale. The abundance of authigenic minerals in the sandstone facies might be related to the distribution of permeability, which might have acted as a conduit for formation water circulation. Except minor amounts of authigenic illite-smectite and illite the shaly facies is dominated by detrital carbonate, quartz and feldspar grains. (3) Part of the silica and carbonate budget for the sandy facies might have come from the interbedded mudstones, siltstones and shaly facies during compaction. The presence of authigenic quartz and carbonate crystals in the sandy facies near the mudstone-sandstone and siltstone-sandstone contacts indicates pore water and mass transfer from the fine-grained sediments. The muddy, silty and shaly facies is frequently interbedded within the East Berlin formation throughout the entire sections. In such stratigraphic settings, part of the ions for the authigenesis of quartz and carbonate cements possibly derived from the interbedded mudstones, siltstones and shales. (4) Gravity-driven acidic meteoric water in the diagenetic environment plays a significant role in leaching and circulating ions downwards in the rift basin, to precipitate different authigenic minerals in the East Berlin formation. In rift basins, gravity-driven meteoric water flow can penetrate at least several kilometers into the sedimentary basin. Pore water migration depends upon permeability distribution and pressure differentials. (5) Clay minerals existed in four forms: (i) mechanically infiltrated clay originating from percolation of mud-rich waters or illuviation of clay cutans, (ii) pedogenic mud aggregates, (iii) transformational clay, i.e. changing of mechanically infiltrated clay to authigenic clay, and

(iv) neoformed clay directly precipitated from the pore water. There is a variation in authigenic clay mineralogy. Illite abundantly distributed in the fluvial sequence whereas smectite-chlorite, illite-smectite and chlorite dominated in the lacustrine sandstones. (6) There are variations in carbonate cements in the studied sandstone formations. Dolomite, ferroan dolomite and ankerite were restricted to the lacustrine sandstones, indicating that saline alkaline conditions were suitable for precipitation. Abundance of calcite found in the fluvial sandstones possibly indicates open drainage. (7) Oil emplacement possibly affected further precipitation of authigenic clay minerals. However, the presence of pyrite and apatite within the bitumen indicate co-precipitation during oil emplacement

ACKNOWLEDGEMENTS

Earlier drafts of this manuscript were read by Dr. J. Parnell and his comments are gratefully acknowledged. Thanks are also extended to Dr. E. Gierlowski-Kordesch, and Dr. A. Ruffell. Most of the work was carried out at the School of Geosciences, the Geochemical Laboratory and the Electron Microscopy Unit, the Queen's University of Belfast. Thanks extended to the staff of these institutions. This research work was financially supported by the School of Geosciences, the Queen's University of Belfast, UK.

REFERENCES

1. Gierlowski-Kordesch, E. Rust, B.R. *Sedimentology and Geochemistry of Modern and Ancient Saline Lakes*, Renaut, R.W.; Last, W.M. (Eds.); SEPM Special Publication 50, Society of Economic Paleontology and Mineralogy: Tulsa, Oklahoma, USA; **1994**, pp 249-265.
2. Bjorlykke, K. *Diagenesis, I, Development in Sedimentology*, Chilingarian, G.V.; Wolf, K.H. (Eds.); Elsevier: Amsterdam; **1988**; 41, pp 555-588.
3. Helmold, K.P.; Van de Kamp, P.C. *Clastic Diagenesis*, McDonald, D.A.; Surdum, R.C. (Eds.); AAPG Memorial 37, American Association of Petroleum Geologists: Oklahoma, USA; **1984**; pp 239-276.
4. Curtis, C.D. *J. Geol. Soc. London* **1978**, 135, 107.
5. Curtis, C.D. *Petroleum Geochemistry and Exploration of Europe*, Brooks, J. (Ed.); *Geol. Soc. Spec. Pub. London* 12, Geological Society of London: London, UK; **1983**; pp 113-125.
6. Bjorlykke, K. *Sediment Diagenesis*, Vol. 115, Parker, A.; Sellwood, B.W. (Eds.); D. Reidel Publishing Company: Dordrecht, Holland; **1983**; pp 169-213.
7. Ahmed, W. *Ph.D. Thesis*, The Queen's University of Belfast, Belfast; UK; **1997**; p 238.
8. Power, M.C. *AAPG* **1967**, 51, 1240.
9. Fuchtbauer, H. *Sediment Diagenesis*, Vol. 115, Parker, A.; Sellwood, B.W. (Eds.); D. Reidel Publishing Company: Dordrecht, Holland; **1983**; pp 269-288.
10. Baker, J.C. *Sedimentology* **1991**, 38, 819.
11. Purvis, K. *Sedimentary Geology* **1992**, 77, 155.
12. Ahmed, W. *Bull. Chem. Soc. Ethiop.* **2002**, 16, 37.
13. Demicco, R.V.; Gierlowski-Kordesch, E. *Sedimentology* **1986**, 33, 107.
14. Manspeizer, W. *Triassic-Jurassic Rifting: Continental Break-up and the Origin of the Atlantic Ocean and Passive Margin*, Manspeizer, W. (Ed.); Part A, Elsevier: Amsterdam; **1988**; pp 41-80.
15. Lorenz, J.C. *Triassic-Jurassic Rift-basin Sedimentology: History and Methods*, Van Nostrand Reinhold: New York; **1988**; p 315.

16. Schlische, R.W. *Tectonics* **1993**, 12, 1026.
17. Smoot, J.P. *Palaeogeography, Palaeoclimatology, Palaeoecology* **1990**, 84, 369.
18. Hubert, J.F.; Feshbach-Meriney, P.E.; Smith, M.A. *AAPG* **1992**, 76, 1710.
19. Gierlowski-Kordesch, E.; Huber, P. *Lake sequences in the central Hartford Basin*: Newark Supergroup: State Geological and Natural History Survey: Connecticut, USA; **1995**; Guidebook 7, B1-B39.
20. Sedemann, D.E. *Am. J. Sci.* **1989**, 289, 553.
21. Hubert, J.F.; Hyde, M.G. *Sedimentology* **1982**, 29, 457.
22. Wenk, W.J. *Northeastern Geology* **1990**, 12, 202.
23. Ellesfsen, K.J.; Simmons, G.; Dowling, J.J.; Dehlinger, P.; Gray, N.H. *Northeastern Geology* **1990**, 12, 231.
24. Walker, T.R. *The Continental Permian in Central, West and South Europe*, Falke, H. (Ed.); D. Reidel Publishing Company: Dordrecht, Holland; **1976**; pp 240-282.
25. Mores, M.A.; De Ros, L. *J. Sed. Petrology* **1990**, 60, 809.
26. Ramos, A. *Geological Magazine* **1995**, 132, 435.
27. Orhan, H. *Sedimentary Geology* **1992**, 77, 111.
28. Giles, M.R.; Marshall, J.D. *Marine and petroleum Geology* **1986**, 3, 243.
29. Bjorlykke, K. *Sedimentary Geology* **1993**, 86, 137.
30. Van de Kamp, P.C.; Leake, B.E. *Chemical Geology* **1996**, 133, 89.
31. Schmidt, V.; McDonald, D.A. *Aspect of Diagenesis*, Scholle, P.A.; Schlunger, P.R. (Eds); SEPM Special Publication 26, Society of Economic Paleontology and Mineralogy: Tulsa, Oklahoma, USA; **1979**, pp 175-207.
32. McBride, M.B. *Environmental Chemistry of Soils*. Oxford University Press: New York, **1994**; p 406.
33. Mullis, A.M. *Sedimentology* **1992**, 39, 99.
34. April, R.H. *Clay and Clay Minerals* **1981**, 29, 31.
35. Tucker, M.E. *Sedimentary Petrology: An Introduction to the Origin of Sedimentary Rocks*, 2nd ed., Blackwell Science Ltd.: London, UK; **1991**; p 260.
36. Cooper, M.K.; Hunter, R.H. *Mineralogical Magazine* **1995**, 59, 213.